Gold Nanoparticles Supported on Functionalized Silica as Catalysts for Alkyne Hydroamination: A Chemico-Physical Insight

Chiara Parise,[a] *Barbara Ballarin,*[a] *Davide Barreca,*[b] *Maria Cristina Cassani,*[a*] *Paolo Dambruoso,*[c] *Daniele Nanni,*[a*] *Ilaria Ragazzini,*[a] *Elisa Boanini*[d]

[a]*Dept. of Industrial Chemistry "Toso Montanari", Bologna University, Viale Risorgimento 4, I-40136, Bologna, Italy;* [b]*CNR-ICMATE and INSTM, Dept. of Chemistry, Padova University, Via F. Marzolo, 1, I-35131, Padova, Italy;* [c]*CNR-ISOF, Via P. Gobetti, 101, I-40129, Bologna, Italy;* [d]*Dept. of Chemistry "Giacomo Ciamician", Bologna University, Via Selmi 2, I-40126, Bologna, Italy.*

*To whom correspondence should be addressed. E-mail: maria.cassani@unibo.it (M.C.C.), fax: +39 051 2093690; tel: +39 051 2093700; daniele.nanni@unibo.it (D.N.), fax: +39 051 2093654; tel: +39 051 2093623.

Abstract

Highly stable gold nanoparticles anchored on propynylcarbamate-functionalized silica (Au/SiO_2@Yne) have been efficiently utilized for the heterogeneous hydroamination of phenylacetylene with aniline under different reaction conditions. In order to ascertain the eventual influence of surface silanol groups on the system activity and selectivity tailored modifications of Au/SiO_2@Yne catalysts were pursued according to two different strategies, involving respectively functionalization with trimethylethoxysilane (Au/SiO_2@Yne-TMS) or post-treatment with tryethylamine (Au/SiO_2@Yne-NEt_3). The prepared materials were analysed by several complementary techniques such as Solid State NMR (SS NMR), Trasmission Electron Microscopy (TEM), X-ray Photoelectron Spectroscopy (XPS), X-ray Diffraction (XRD). A comparison of the resulting catalytic activities with that of the pristine Au/SiO_2@Yne revealed a significant improvement for Au/SiO_2@Yne-NEt_3 in terms of both conversion and selectivity. Recycling and stability studies showed a catalytic activity decrease after the first run, due to the formation of polyphenylacetylene (PPhA) oligomers shielding the active sites. PPhA removal by sonication in acetone fully restored the catalytic activity and empowered the system with a good operational stability, a very crucial issue in view of eventual practical applications.

Keywords: gold nanoparticles, propynylcarbamate-functionalized silica, heterogeneous catalysis, hydroamination, solid state NMR spectroscopy.

1. Introduction

Hydroamination reactions, involving addition of N-H bonds across unsaturated C-C bonds, are of considerable importance in synthetic organic chemistry, since they stand as an atom-economical route to valuable *N*-containing products as constituents of various fine chemicals [1][2][3][4][5][6]. In the case of alkenes, hydroamination products are stable secondary or tertiary amines, whereas alkynes are transformed into reactive species, *i.e.* enamines and imines, that are useful intermediates for multi-step syntheses encompassing, among others, polymerizations, asymmetric hydrogenations [7], cyclo-additions [8], and cross-coupling reactions [9]. As a matter of fact, the addition of an amine to a C-C unsaturated bond is kinetically hampered by the electron repulsion between the multiple bond π system and the electron density located on nitrogen, resulting in a high activation barrier [10]. Non-catalytic hydroaminations involve the use of strong acids to protonate the C−C multiple bond, facilitating the amine attack [11][12][13], or strong bases to generate strongly nucleophilic amido species, which react more easily with C−C moieties [14][15][16]. As a consequence, a great deal of efforts have been recently focused on the development of efficient metal-based catalysts for this type of reactions [10][17][18][19].

Among transition metals, gold shows an affinity towards C≡C bonds which is by far the highest one [20][21]. In fact, Au is sometimes referred to as "*alkynophile*" for its remarkable ability to preferentially coordinate C-C triple bonds even in the presence of other functional groups, making the substrate more reactive towards nucleophilic attack. In particular, gold-catalyzed alkyne activation has been generally performed using homogenous Au(I) complexes [22][23], but more recently research on the use of supported gold nanoparticles (AuNP) based heterogeneous catalysts has flourished [1][3][24][25][26][27].

In this framework, our research group has developed a convenient method for the anchoring, without the addition of any external reducing and/or stabilizing agent, of AuNP on different oxide supports (SiO_2, Al_2O_3, TiO_2, Fe_3O_4) previously modified with a propynylcarbamate organic functionality [28][29]. Among the investigated systems, the Au/SiO_2@Yne one (where Yne stands

for alkyne) demonstrated to be very robust and active in the oxidation of various primary and secondary alcohols [28]. These findings prompted us to explore its catalytic behaviour in alkyne hydroamination processes, which is the main aim of the present research work. In order to ascertain how the presence of silanol groups (≡Si-OH) on the silica surface could affect the process activity and selectivity [30], Au/SiO_2@Yne catalysts were subjected to chemical modifications according to two different strategies. In the first approach, the functionalized silica SiO_2@Yne was reacted with ethoxytrimethylsilane (TMS) before treatment with $HAuCl_4$, whereas in the second one Au/SiO_2@Yne was post-treated with NEt_3 solutions. The obtained systems (Au/SiO_2@Yne-TMS and Au/SiO_2@Yne-NEt_3, respectively) were subjected to a detailed chemico-physical characterization by means of complementary analytical techniques. Finally, their catalytic activity in the hydroamination of phenylacetylene with aniline was studied, critically comparing the observed performances in comparison with the ones pertaining to Au/SiO_2@Yne. As discussed below, functionalization with NEt_3 and post-treatments by means of acetone sonication were proved to be key steps in order to avoid detrimental losses of catalytic performances.

2. Results and Discussion

2.1 Catalyst Preparation and Characterization

The new catalysts Au/SiO_2@Yne-TMS and Au/SiO_2@Yne-NEt_3 were prepared by employing the two different strategies shown in Scheme 1: *a)* silanization with ethoxytrimethylsilane (TMS) of the functionalized silica SiO_2@Yne, followed by reaction with a 1.0 mM aqueous solution of chloroauric acid to accomplish the *in situ* Au(III) → Au(0) reduction; *b)* impregnation of the formerly prepared Au/SiO_2@Yne with a 3 v/v % solution of triethylamine in anhydrous toluene [31].

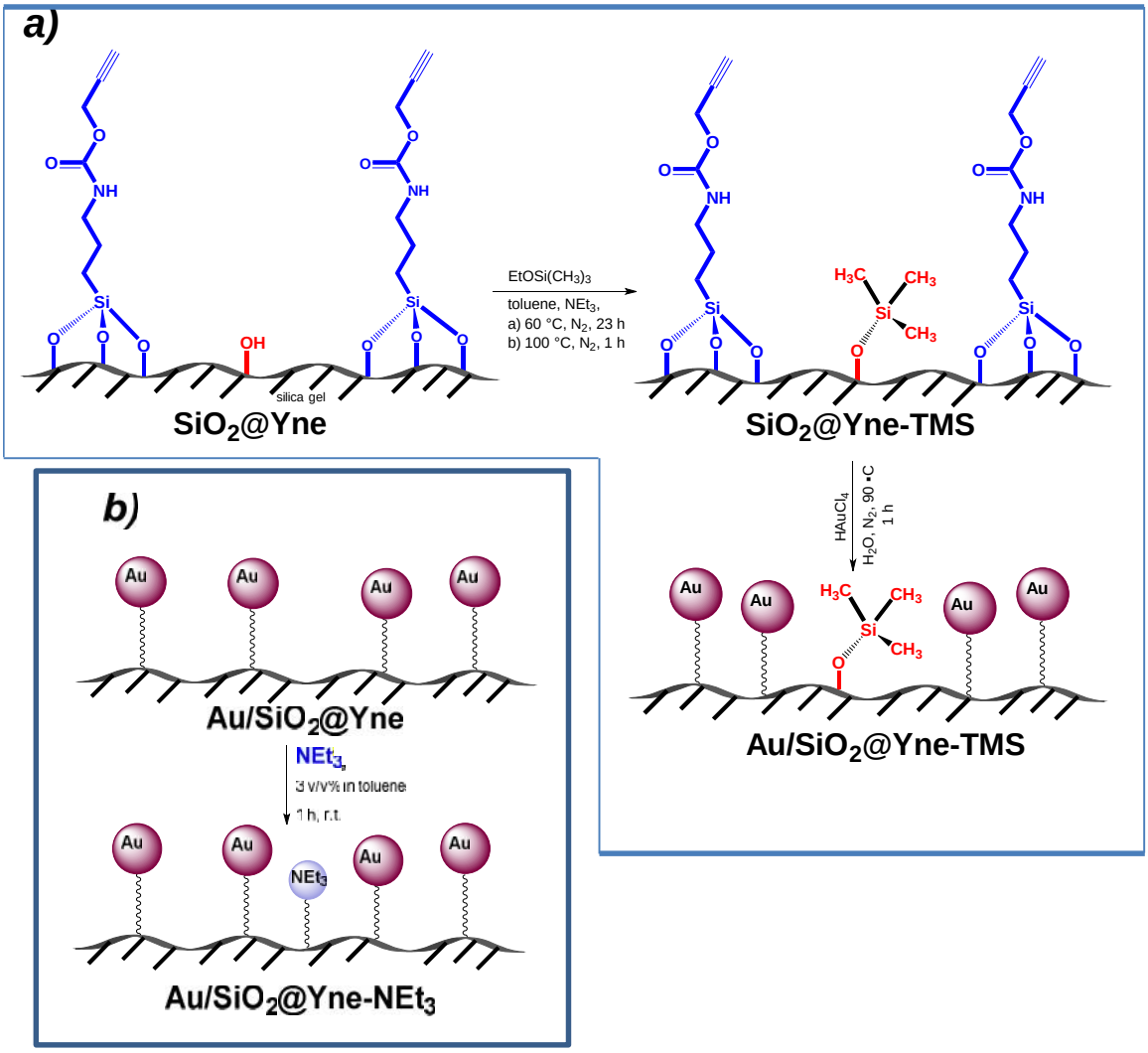

Scheme 1. Sketch of the preparation routes adopted in the present work for the synthesis of Au/SiO_2@Yne-TMS and Au/SiO_2@Yne-NEt_3 catalysts.

Each step described in Scheme 1 was monitored by SS NMR spectroscopy (Fig. 1).

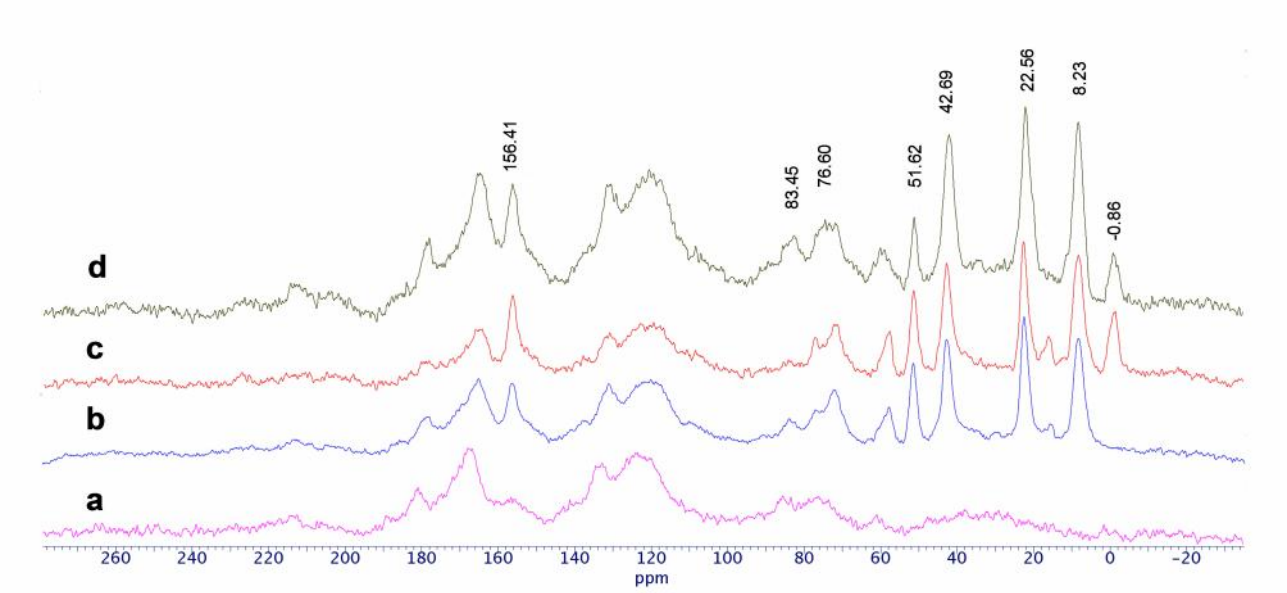

Fig. 1. ^{13}C CP-MAS NMR spectra recorded at 500 MHz of a) bare silica, b) SiO_2@Yne, c) SiO_2@Yne-TMS, d) Au/SiO_2@Yne-TMS.

The large signals in the regions 70 – 90 ppm, 110 -140 ppm, and 160 – 180 ppm belong to impurities contained in the commercial silica substrate (Fig. 1a), whereas the signals due to the propynylcarbamate moiety are located at 8.23, 22.56, and 42.69 ppm (propylic chain), 51.62 ppm (propargyl methylene), 76.60 and 83.45 ppm (alkyne carbons), and 156.41 ppm (carbamic carbonyl, Fig. 1b) [28]. The spectrum of SiO_2@Yne-TMS presents an additional peak at -0.86 ppm, ascribable to the $–Si(CH_3)_3$ group introduced in the additional functionalization step (Fig. 1c) [32]. The presence of gold anchored on the support results in a slight intensity decrease of the peaks associated to propynylcarbamate partial oxidation occurring during Au(III) reduction (Fig. 1d) [28].

Fig. 2 compares representative SS NMR spectra in the range 0 ÷ 60 ppm (the full spectra are reported in Fig. S1) of systems obtained after different functionalization processes. The comparison of the chemical shifts of NEt_3 adsorbed on bare silica (6.82 and 44.41 ppm, Fig. 2a) with the

pertaining ones in solution (^{1}H-NMR in $CDCl_3$: 11.78 and 46.46 ppm) evidenced the interaction between the silica surface and the amine, which was more pronounced on the low frequency signal [33]. The presence of an adsorbed Lewis base was clearly confirmed in the spectrum of SiO_2@Yne-NEt_3, although the two peaks were partially overlapped with the propylic chain ones (Fig. 2b). In a different way, the triethylamine resonances could not be unambiguously identified in the case of Au/SiO_2@Yne-NEt_3 (Fig. 2c), likely due to a complete overlap of the signals.

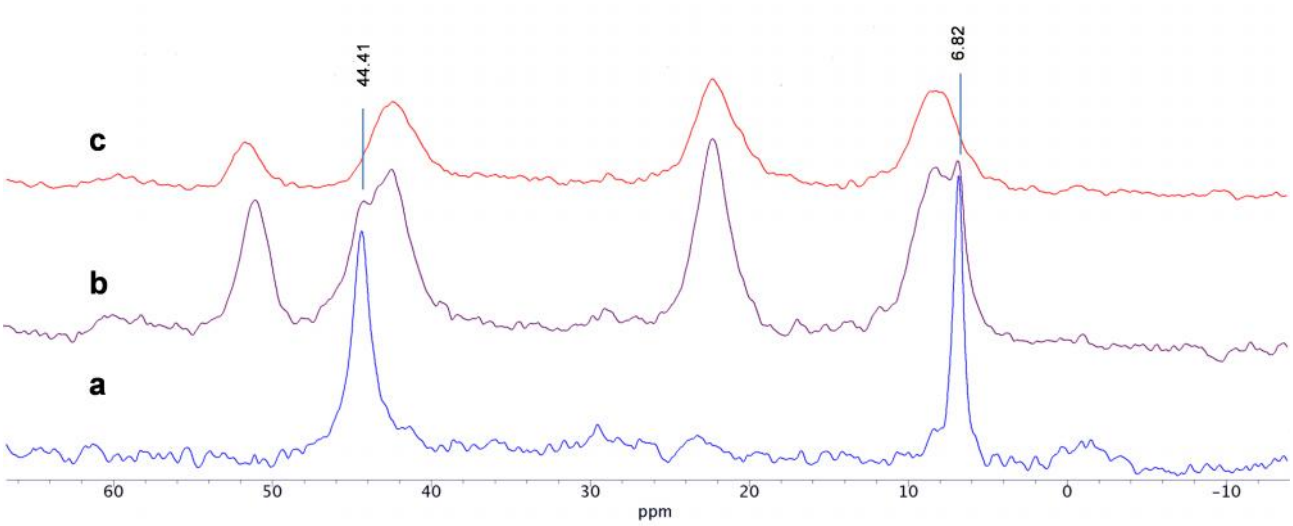

Fig. 2. ^{13}C CP-MAS NMR spectra recorded at 500 MHz of a) SiO_2-NEt_3 b) SiO_2@Yne-NEt_3, c) Au/SiO_2@Yne-NEt_3.

The catalysts were successively thoroughly characterized by other complementary techniques and some of the data are summarized in Table 1 (for comparison the data previously obtained for Au/SiO_2@Yne are also reported).

Table 1. TGA, AAS, and TEM data.

Sample	Yne (wt %)[a]	Au (wt%)[b]	AuNP d_{TEM} (nm)
Au/SiO_2@Yne[c]	12 ± 1	3.7 ± 0.1	15 ± 4
Au/SiO_2@Yne-TMS	13 ± 1	4.4 ± 0.1	33 ± 10
Au/SiO_2@Yne-NEt_3	12 ± 1	4.4 ± 0.1	14 ± 5

[a]weight loss in the temperature range (200 – 750 °C) by TGA; [b]determined by AAS; [c]ref. 28.

The weight loss of the organic material in the temperature range (200 – 750 °C) for Au/SiO_2@Yne-TMS (Fig. S2c) was 13 wt %, in keeping with the introduction of the trimethylsilane group on the silica surface. Conversely, the Au/SiO_2@Yne-NEt_3 thermogram (Fig. S3c) differed from that of Au/SiO_2@Yne only for a 2 wt% in the 96 – 200 °C temperature range, attributed to the presence of the amine physisorbed on silica (see also Fig. S3a). The gold content in Au/SiO_2@Yne-TMS and Au/SiO_2@Yne-NEt_3 indicated a weight percentage of gold anchored on the support comparable to the one previously found for Au/SiO_2@Yne. These results suggested that additional modifications of the silica surface do not affect the gold amount immobilised by means of the propynyl-carbamate functionality.

The morphology and nanostructure of the gold nanoparticles anchored on the new supports were investigated by TEM. The analysis of the Au/SiO_2@Yne-TMS sample indicated the presence of spherically shaped AuNP with an average size of (33 ± 10) nm (Fig. 3a), significantly larger than the ones present in the Au/SiO_2@Yne catalyst [(15 ± 4) nm)]. On the contrary, TEM images of Au/SiO_2@Yne-NEt_3, showed that the treatment with triethylamine did not affect the size of the previously immobilised AuNP (14 ± 5 nm; Fig. 3b).

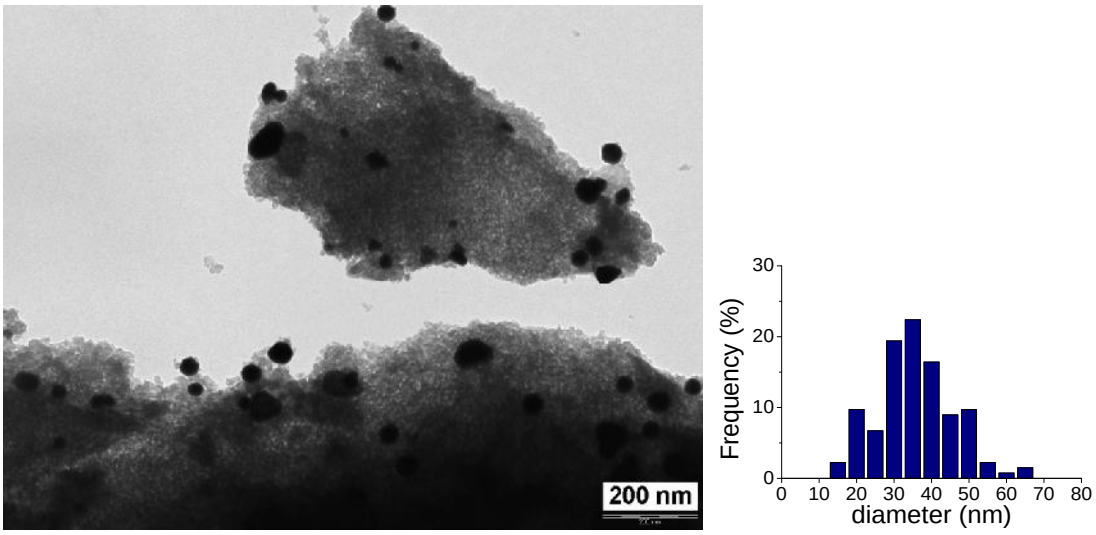

(a)

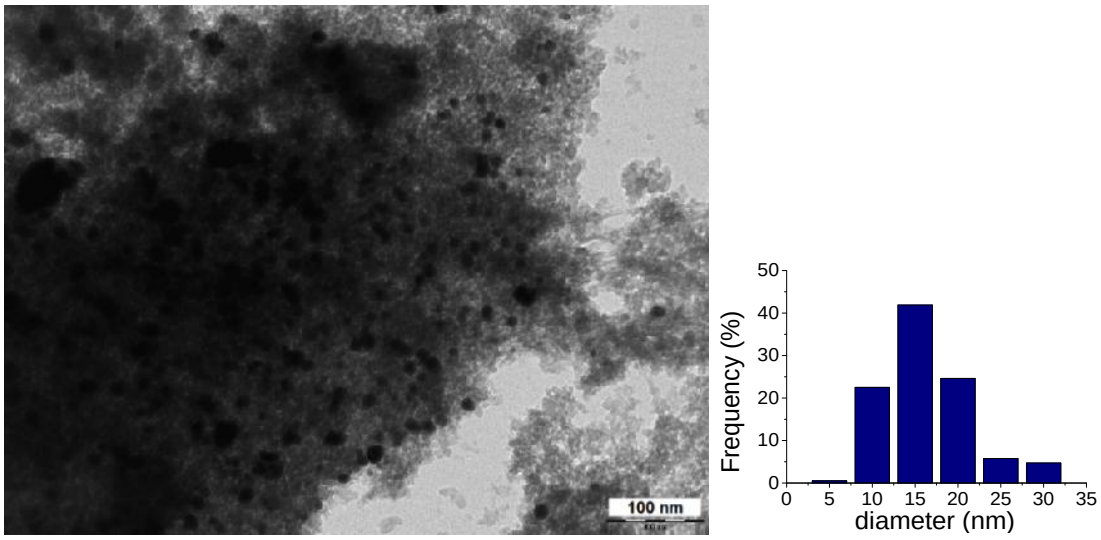

(b)

Fig. 3. Representative TEM images and particle size distribution of a) Au/SiO_2@Yne-TMS and b) Au/SiO_2@Yne-NEt_3.

Microstructural information was obtained by XRD analyses (Fig. 4), which revealed not significant differences between the patterns recorded on Au/SiO_2@Yne, Au/SiO_2@Yne-TMS, and Au/SiO_2@Yne-NEt_3. The diffraction peaks at 2θ = 38.13°, 44.33°, 64.56°, and 77.55° indicate the presence of metallic Au as the sole crystalline phase (JCPDS no. 03-065-2870) and refer to (111), (200), (220), and (311) crystallographic planes, respectively. Silica was always present as an amorphous phase, which is clearly appreciable in the broad halo in the 15-35° angular range.

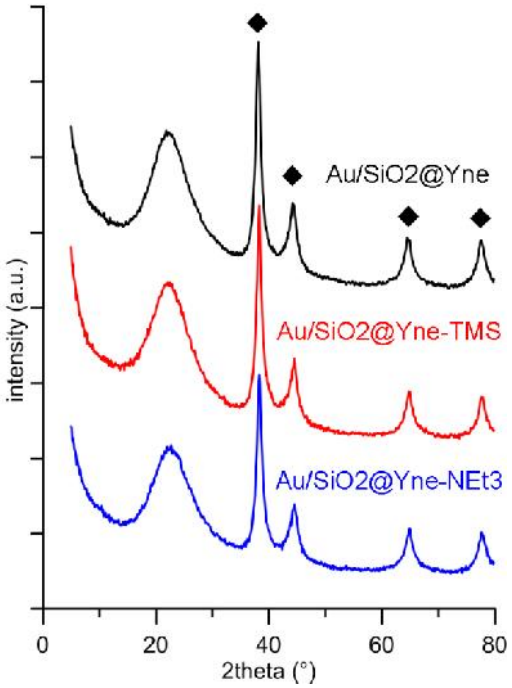

Fig. 4. XRD patterns of Au/SiO_2@Yne, Au/SiO_2@Yne-TMS, Au/SiO_2@Yne-NEt_3. Peaks due to metallic gold are indicated with ♦.

XPS analyses were used to assess the surface chemical composition of the target specimens before and after catalytic tests. Survey spectra (Fig. 5a) were dominated by the presence of C, O, N, Au, and Si photopeaks, and no impurity signals were observed.

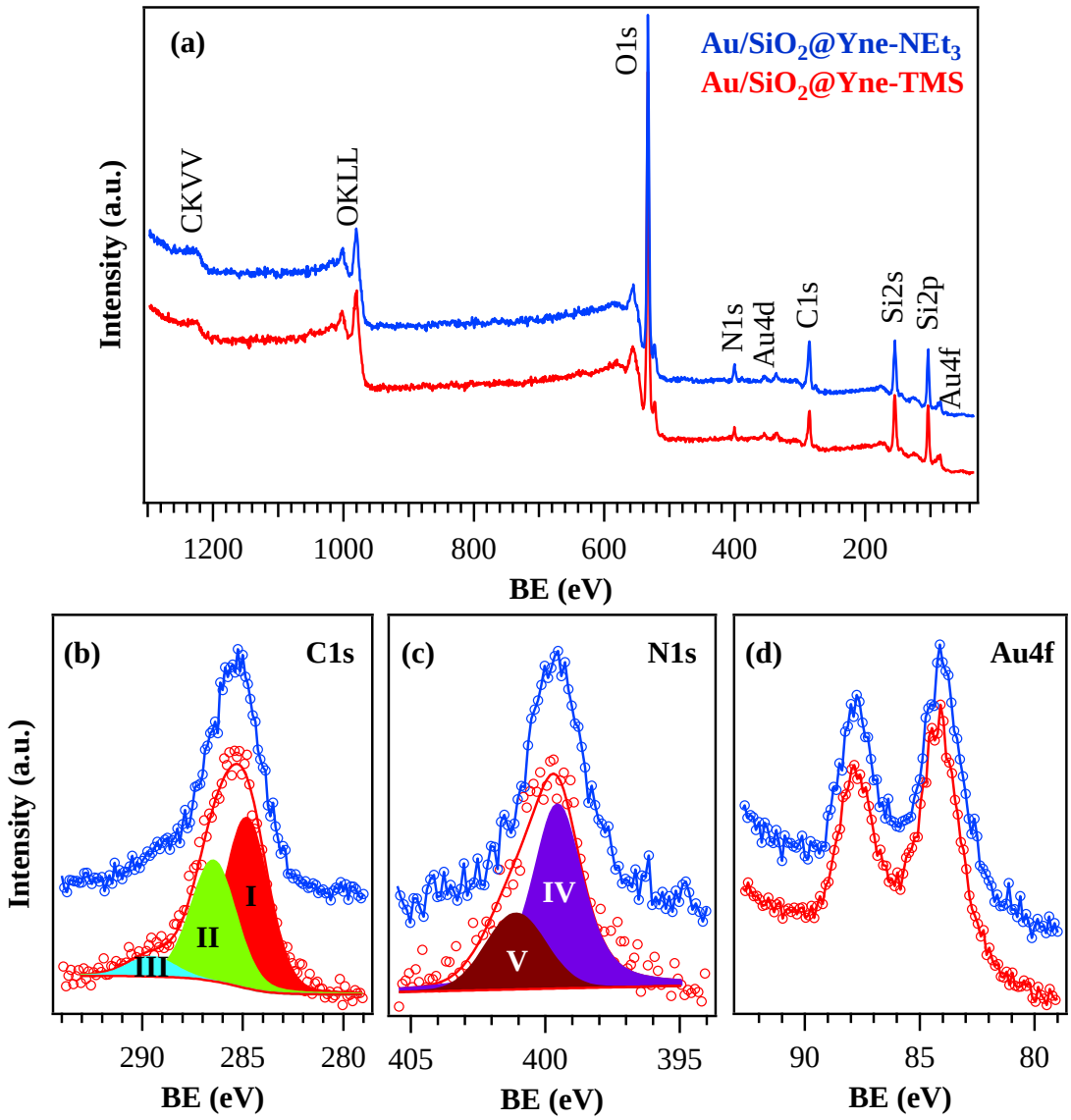

Fig. 5. Surface wide-scan XPS spectra (a) and C1s (b), N1s (c), and Au4f (d) photoelectron peaks for as-prepared samples.

For the as-prepared specimens, the C1s peak (Fig. 5b) could be deconvoluted by means of three distinct components located at average BE values of 284.8 eV (**I**, ≈53% of the total carbon signal), 286.4 eV (**II**, ≈40% of the total carbon signal), and 289.4 eV (**III**, ≈7% of the total carbon signal). The main peak (**I**) resulted from the concurrent contributions of adventitious carbon due to air exposure, as well as of C–C, C–H, and/or C–Si moieties from the ligand chains. In a different way, component **II** corresponded to C–X bonds (X = N or O), and band **III** could be attributed to O–C=O groups from the carbamate moieties [34][35][36][37]. The contribution of adventitious

carbon to component **I** prevented from a more detailed discrimination of the various concurrent species [28]. Two bands contributed to the N1s signal (Fig. 5c), a principal one, due to N in amino-groups (**IV**, BE = 399.4 eV), and an additional one, attributable to NH–COO– moieties (**IV**, BE = 401.1 eV) [28][35][37]. As expected, the relative weight of contribution **IV** increased from ≈72 to ≈80% upon going from Au/SiO_2@Yne-TMS to Au/SiO_2@Yne-NEt_3, due to the presence of NEt_3 groups. As far as the Au 4f peak is concerned (Fig. 5d), the BE values [BE($Au4f_{7/2}$) = 84.1 eV, BE($Au4f_{5/2}$) = 87.8 eV] were characteristic of metallic Au and enabled to discard the presence of Au(I) and/or Au(III) species in appreciable amounts [36][38][39][40]. The typical surface Au content was estimated to be 0.3 – 0.4 at.%, corresponding to an Au/Si at.% ratio of 0.02. The surface O1s and Si2p signal positions (Fig. S4; BE = 532. 5 eV and BE = 103.0, respectively) were consistent with the presence of a SiO_2-like network [28][35][37]. As regards O1s, the presence of concomitant contributions from –OH groups from air exposure and of oxygen atoms in the ligand chains with BE very close to that of oxygen in SiO_2 was responsible for the measured O/Si at.% ratio (≈2.6), higher than the value expected for stoichiometric SiO_2 [28][34][35][40].

2.2 Hydroamination of phenylacetylene with aniline

The catalytic activity of the target systems (Au/SiO_2@Yne, Au/SiO_2@Yne-TMS, and Au/SiO_2@Yne-NEt_3) was investigated in alkyne hydroamination processes, choosing as a model reaction the hydroamination of phenylacetylene with aniline, which, in the present study, always led to the regioselective formation of the Markovnikov product phenyl(1-phenylethylidene)amine.

The effect of experimental parameters such as solvent, reaction temperature, reagents molar ratio, and the presence of acid additives was evaluated using Au/SiO_2@Yne, and the results are summarized in Table 2. The best results in terms of conversion were observed in solvent-free conditions at 110 °C for 24 h, with a catalyst loading of 1.0 % mol Au (entries 1-3). Since a change in the molar ratio of phenylacetylene to aniline, while keeping the temperature and the amount of

catalyst constant (w.r.t. the limiting reagent), did not lead to significant conversion and selectivity variations (entries 2,3), a 1:1 molar ratio was employed in all the subsequent experiments.

In view of a possible future use in continuous flow packed bed reactors, we also examined the behaviour of our catalyst in toluene, ethanol, and acetonitrile with the reagents in 1.0 M concentration (entries 6, 8-9). In line with literature data [38], toluene was found to be the best performing solvent (see also Table 3), although with conversions lower than in solvent-free conditions, and no significant differences were found by using 1.0 M or 0.5 M concentrations (entry 7). Finally, basing on previous works on the activation of gold-based catalysts for alkyne hydroamination by acid promoters [3][41][42][43][44], attention was also devoted to the effects of two acid additives, *i.e.* phosphotungstic acid ($H_3PO_4 \cdot 12WO_3$) and silica sulfuric acid additive SiO_2-OSO_3H. Despite these systems favourably affected the obtained conversions, this positive effect was counterbalanced by a significant selectivity decrease.

Table 2. Au/SiO_2@Yne-catalyzed hydroamination of phenylacetylene with aniline.[a]

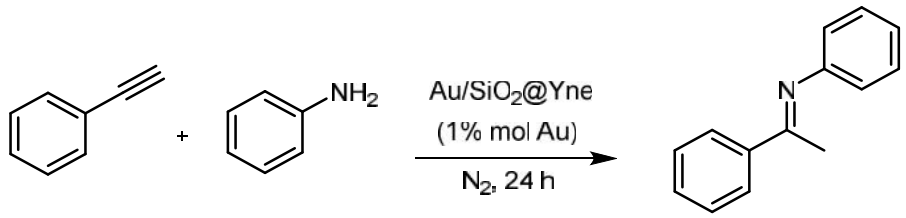

FA AN IMM

Entry	Solvent	FA:AN	Additive (mol% w.r.t. Au)	T (°C)	Conv (%)[b]	Φ_{IMM} (%)[b]
1	no solvent	1:1	-	110	91	90
2	no solvent	1.5:1	-	110	93	88
3	no solvent	1:1.5	-	110	95	81
4	no solvent	1:1	-	80	71	82
5[c]	no solvent	1:1	-	110	54	90
6	toluene	1:1	-	110	78	88
7[d]	toluene	1:1	-	110	76	95
8	ethanol	1:1	-	80	22	42
9	CH_3CN	1:1	-	80	46	>99
10[e]	toluene	1:1	-	110	-	-
11	toluene	1:1	$H_3PO_4 \cdot 12WO_3$ (0.5)	110	89	74
12	toluene	1:1	SiO_2-OSO_3H (0.5)	110	86	68

[a] Reaction conditions: 1.0 M concentration, 1 mL scale. [b] Conversion (Conv) and selectivity (Φ_{IMM}) were determined by GC-MS analysis using 1,3,5-TMB as internal standard (absolute error: ± 5%), values are averages of three runs. [c] 0.5 % mol Au, [d] 0.5 M concentration. [e] blank test carried out in the absence of Au/SiO_2@Yne.

Subsequently, the activity of Au/SiO_2@Yne-TMS and Au/SiO_2@Yne-NEt_3 catalysts was investigated under the conditions described in Table 3 and compared with that of Au/SiO_2@Yne. It is worth to underline that since we used a 1 % mol content of Au, the Turn Over Numbers (TON) in our case correspond to the converted substrate percentages reported in Table 3.

Table 3. Hydroamination of phenylacetylene with aniline catalyzed by Au/SiO_2@Yne, Au/SiO_2@Yne-TMS, and Au/SiO_2@Yne-NEt_3.[a]

Entry	Catalyst	t (h)	Conv (%)[b]	Φ_{imm} (%)[b]
1	Au/SiO_2@Yne	5	50	93
2	Au/SiO_2@Yne-TMS	5	51	95
3	Au/SiO_2@Yne-NEt_3	5	48	>99
4	Au/SiO_2@Yne	24	78	82
5	Au/SiO_2@Yne-TMS	24	83	86
6	Au/SiO_2@Yne-NEt_3	24	98	96
7	Au/SiO_2@Yne	24	65	85
8	Au/SiO_2@Yne-NEt_3	24	85	92
9	Au/SiO_2@Yne + 3 % v/v NEt_3[c]	24	65	88
10	Au/SiO_2@Yne-NEt_3 reuse 1	24	70	83
11	Au/SiO_2@Yne reuse 1	24	70	88

[a] Reaction conditions: 1:1 stoichiometric ratio of phenylacetylene/aniline and 1.0 M reagents concentration, T = 110 °C, N_2 atm, 1 % mol Au; entries 1-6: 1 mL scale; entries 7-11: 10 mL scale. [b] Conversion (Conv) and selectivity (Φ_{IMM}) were determined by GC-MS (absolute error: ± 5%), values are averages of three runs; [c] 3 % v/v NEt_3 was added in the reaction mixture.

After 5 h, the results obtained in terms of both conversion and selectivity were found to be comparable for the three catalysts (entries 1-3). In particular, whereas the conversion achieved was ≈50 %, the occurrence of side reactions leading to acetophenone formation was found to be negligible, resulting in a very high selectivity towards the imine product [45]. After 24 h, all the conversions underwent a significant increase (entries 4-6). Nevertheless, while no significant differences were observed in the catalytic performance of Au/SiO_2@Yne and Au/SiO_2@Yne-TMS, a remarkable rise up to 98 % was observed for Au/SiO_2@Yne-NEt_3 (96 % selectivity in imine). This result is even better than those reported by Corma et al. for AuNP on hybrid chitosan-SiO_2 under conditions similar to ours [24]. The highest selectivity observed under these conditions, in our opinion, could be also ascribable to neutralization of the silanols acidic sites present on the silica, which could in principle favour hydrolysis of the imine. Indeed this observation is in agreement with the data reported in Table 2, entries 11 and 12, where the presence of acidic additives such as phosphotungstic acid and silica sulfuric acid decrease the reaction selectivity.

When the reaction was carried out with 300 mg of catalyst instead of 30 mg, a slight decrease in the conversion values for Au/SiO_2@Yne and Au/SiO_2@Yne-NEt_3 was observed, though the trimethylamine-modified catalyst still displayed a 20% higher activity (entries 7-8). In consideration of these results, an additional experiment was performed with NEt_3 added directly into the reaction environment. Therefore, a suspension of Au/SiO_2@Yne was stirred at room temperature in a 3 % v/v solution of triethylamine in toluene for 30 min before adding the reagents and heating at 110 °C; though, no significant enhancement of the resulting conversion was observed (entry 9).

As Au/SiO_2@Yne-NEt_3 was found to be the most active system in the target reaction, recycling tests were initially carried out with this catalyst. After the first reaction run the catalyst was recovered by centrifugation, washed with toluene, and dried before re-use, leading to a conversion decrease by 40-50 %. In a different way, when the exhausted catalyst was instead sonicated in acetone for 30 min, the conversion obtained in the second run was found to be ≈70 %

(entry 10), that is the same obtained with fresh Au/SiO_2@Yne. TGA and XPS analysis carried after treating the exhausted Au/SiO_2@Yne-NEt_3 with acetone/US suggest that this behaviour is due to the loss of the adsorbed triethylamine after the first cycle of reaction. In fact, no weight loss was present in the range 100 – 200 °C in the TGA profile (Fig. S5), whereas in the XPS analysis (Fig. S6) the C content (≈20.0 at.%) was found to be decreased with respect to the pristine Au/SiO_2@Yne-NEt_3 (≈26.0 at.%), and a similar drop was observed for the contribution **IV** (N in amino-groups) in the N1s photoelectron peak (≈75% at.%) compared to the fresh Au/SiO_2@Yne-NEt_3 (≈80%).

A similar reduction in the catalytic activity after the first cycle was observed with Au/SiO_2@Yne, and sonication in acetone proved to be effective in restoring the initial catalytic activity, (entry 11) which remained constant after five cycles of reaction. ^{1}H NMR, IR, GPC (Fig. S7) and ESI-MS (Fig. S8) analysis of the acetone washings indicated the presence of polyphenylacetylene (PPhA) oligomers. The ^{1}H NMR spectra revealed the characteristic peak at 6.09 ppm associated to the vinyl protons of the PPhA chain, alongside with the multiplets at 6.60 ppm and 7.05 ppm corresponding to aromatic protons [46][47][48][49]. Consistently with these results, the IR spectra presented bands at 696 cm^{-1}, 754 cm^{-1}, 849, cm^{-1}, and 1443 cm^{-1} associated to PPhA [50]. The formation of PPhA oligomers in the reaction environment and their consequent adsorption on the catalyst surface is likely to be responsible for poisoning of the active sites and for the drastic reduction of the catalytic performances after the first run. XPS analyses carried on Au/SiO_2@Yne recovered after the first reaction run and simply washed with toluene yielded results in qualitative agreement with those pertaining to the fresh samples (Fig. S6). This result indicated the presence of the same chemical species and enabled to discard the occurrence of significant compositional alterations after functional tests. Nevertheless the increase in the overall carbon content with respect to Au/SiO_2@Yne-TMS (≈25.0 at.% *vs.* ≈18.0 at.%) was in line with the presence of PPhA.

The AAS analysis on the catalyst used for five runs after acetone/sonication treatment, showed that the gold loading was the same as the fresh one. In addition, TEM analysis did not reveal any significant morphological alteration (Fig. S9), hence highlighting the robustness of our silica-supported catalytic systems [24].

Additional insights into the Au/SiO_2@Yne functional behaviour was gained by investigating the reactions with different alkynes and anilines (Table 4). All the reported conversions were measured after 5 h.

Table 4. Substrate scope with the catalyst Au/SiO_2@Yne.[a]

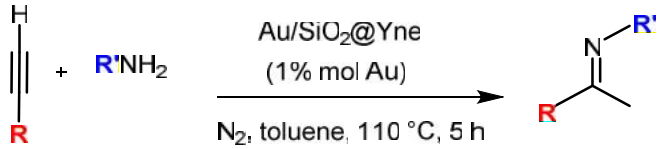

Entry	Alkyne	Amine	Conv (%)[b]	Φ_{imm} (%)[b]
1	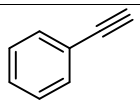	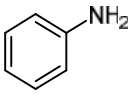	50	93
2	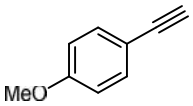	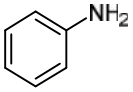	66	89
3	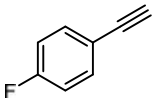	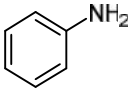	42	87
4	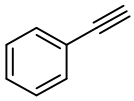	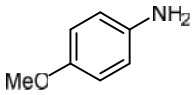	34	93
5	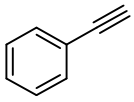	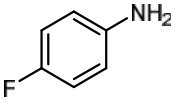	67	95
6	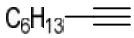	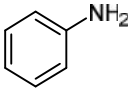	38	69

[a] Reaction conditions: alkyne (1 mmol), amine (1 mmol), 1 % mol Au, toluene (1 mL), t = 5 h, N_2; [b]conversion and selectivity were determined by ^{1}H-NMR analysis using 1,3,5-TMB as internal standard.

As a matter of fact, the conversion of the hydroamination reaction was favoured either by the presence of an electron donating group, such as a methoxy group, on the alkyne (entry 2), or by the presence of an electron-withdrawing group on the aniline ring (entry 5). The electron-donating or -withdrawing ability of the substituents did not have instead any influence on the regioselectivity of the reaction, that remained Markonikov in all cases. These findings, especially as far as the aniline behaviour is concerned, are in good agreement with those reported by Zhu [1] and with the presence of positively charged AuNP on the surface of our catalysts [28]. This, from a mechanistic point of view, clearly points to the formation of electrophilic amine species attacking electron-rich alkynes.

Conclusions

This work was focused on the fabrication and chemical functionalization of gold NP-based systems for applications as heterogeneous catalysts in hydroamination reactions. In particular, efforts were devoted to the modification of Au/SiO_2@Yne systems by either pre-grafting with ethoxytrimethylsilane of the functionalized support SiO_2@Yne, or post-treatment with triethylamine. The resulting Au/SiO_2@Yne-TMS and Au/SiO_2@Yne-NEt_3 materials were characterized in detail by several complementary techniques, to gain a thorough picture of their chemical and physical properties. Taken together, the results showed that the surfaces of all catalysts were decorated with pure Au nanoparticles, and no signals related to Au(I) and Au(III) species could be identified. The presence of a trimethylsiloxane group on the silica surface led to the formation of larger AuNP (33 nm *vs.* 15 nm), whereas no changes in size was observed upon post-treatment with triethylamine. The catalytic activity in the hydroamination reaction of phenylacetylene with aniline showed that the freshly prepared Au/SiO_2@Yne-NEt_3 was the best performing one in terms of conversion and selectivity, whereas no significant differences were observed for Au/SiO_2@Yne-TMS. The results obtained with Au/SiO_2@Yne-NEt_3 were comparable to, sometimes even better than, those reported in the literature for other heterogeneous AuNP-

catalyzed hydroaminations. Recycling and stability studies showed that the positive effect of having a physisorbed base is lost after the first catalytic run, and that the occurring activity loss could be associated with the formation of polyphenylacetylene (PPhA) oligomers poisoning the active sites. Elimination of PPhA by sonication in acetone fully restored the catalytic activity, that remained constant for five consectutive runs, thus confirming the robustness of such catalytic systems. To date, preliminary experiments on possible applications of these catalysts to continuous-flow-conditions gave interesting selectivities (ca. 80%) but low conversions (below 50%); studies are underway to optimize the results and to extend the scope of the reaction.

Experimental Section

Materials. Ethoxytrimetylsilane (98%), Triethylamine (TEA, 99%), Phenylacetylene (98 %), 4-ethynyltoluene (97 %), 4-ethynylanisole (97 %), 1-ethynyl-4-fluorobenzene (99 %), 1-octyne (97 %), aniline (99 %), 4-fluoroaniline (99 %), 4-methoxyaniline (99 %), phosphotungstic acid hydrate ($H_3PO_4 \cdot 12WO_3 \cdot xH_2O$), acetophenone (99 %), phenyl-(1-phenylethylidene)amine (98 %), 1,3,5-trimethoxybenzene (1,3,5-TMB, 99 %), ethanol (EtOH, 99 %), acetonitrile (CH_3CN, 99 %), chloroform ($CHCl_3$, 99 %), deuterated chloroform ($CDCl_3$), sulphuric acid (H_2SO_4, 99%), chloridric acid (HCl, 37 wt%), nitric acid (HNO_3, 65 wt%), sodium hydroxide (NaOH, 50 wt%), of analytical reagent grade were used as purchased from Sigma-Aldrich. Toluene was dried over Na/K alloy, distilled under nitrogen prior to use and stored under inert atmosphere on 4 Å molecular sieves; chloroform used in the GC-MS analysis was stored under nitrogen on alumina; ultrapure water purified with the Milli-Q plus system (Millipore Co, resistivity over 18 MΩ cm) was used in all cases. $HAuCl_4 \cdot 3H_2O$, SiO_2@Yne and Au/SiO_2@Yne were prepared as previously described [51]. In all cases, the support was commercial silica gel (particle size 70-230 mesh, pore volume c.a. 0.8 cm^3/g, surface area 550 m^2/g, Sigma-Aldrich), pre-heated at 180 °C under a dry nitrogen flow, and stored under nitrogen prior to use [52]. The silica sulfuric acid additive SiO_2-OSO_3H (H_2SO_4 3.0 wt % supported on silica) was prepared by adding 87 µL of H_2SO_4 to 5.0 g of

anhydrous SiO_2 previously suspended in 20 mL of Et_2O [53]. After stirring at room temperature for 10 min and solvent evaporation under vacuum, the obtained solid was dried in oven at 50 °C for 24 h and stored under nitrogen. For comparison, SiO_2-NEt_3 and SiO_2@Yne-NEt_3 samples were prepared as follows. A dry round-bottomed flask was charged with 0.30 g of the anhydrous matrix (SiO_2 or SiO_2@Yne) and 10 mL of a 3 % v/v NEt_3 solution in toluene. After stirring the reaction mixture at room temperature for 1 h and solvent removal under vacuum at 70 °C, the resulting solid was dried in oven at 65 °C for 24 h.

Preparation of Au/SiO_2@Yne-TMS. *First step*: a 3.0 g of SiO_2@Yne were suspended in 40 mL of anhydrous toluene under a nitrogen atmosphere, and subsequently $EtOSiMe_3$ (2 mL, 1.52 g, 12.8 mmol) and TEA (178 µL, 1.28 mmol) were added to the stirred suspension. After heating at 60 °C for 23 h and at 100 ° C for 1 h, the solvent and the silane excess were removed by rotary evaporation, and the resulting white solid (SiO_2@Yne-TMS) was kept overnight at 70 °C, cooled under vacuum and stored under nitrogen. *Second Step*: 2.5 g of SiO_2@Yne-TMS were suspended in 330 mL of water under nitrogen. was After heating to 90 °C and vigorous stirring, 300 mL of aqueous $HAuCl_4 \cdot 3H_2O$ (0.250 g, 0.63 mmol, 1.0 mM final concentration) was rapidly added. The pale yellow colour quickly turned deep purple, and after 1 h the solid was filtrated and thoroughly washed with water and ethanol. After one night at 70 °C, the solid was kept 8 h under vacuum, and the final purple powder (Au/SiO_2@Yne-TMS) (2.63 g) was stored under nitrogen. The gold content (determined by AAS) was (4.3 ± 0.1) wt%.

Preparation of Au/SiO_2@Yne-NEt_3. . After three vacuum/nitrogen cycles applied to 2.0 g of Au/SiO_2@Yne, 90 mL of a 3.0 v/v% TEA solution of in anhydrous toluene were added. The suspension was stirred for 1 h at room temperature and then the surnatant was decanted off. The solid was washed with toluene (3x10 mL), dried by rotary evaporation, maintained at 70 °C overnight,cooled under vacuum and finally stored under nitrogen. The gold content (determined by AAS) was (4.4 ± 0.1) wt%.

Characterization. Detailed information regarding instruments and methods employed for

Thermogravimetry (TGA), Atomic Absorption Spectroscopy (AAS) and GC-MS are reported in the Supplementary Material. Solid State NMR spectra (SSNMR) were recorded using adamantane as reference on an Agilent NMR system, consisting of a 54-mm bore, 11.7 Tesla Premium Shielded superconducting magnet, a DD2 Performa IV NMR console equipped with 100 W highband and 300 W lowband amplifiers, and a NB Agilent 3.2 mm T3 MAS HXY Solid Probe 500 MHz. TEM analyses were performed using a Philips CM 100 transmission electron microscope operated at 80 kV. To prepare samples for TEM observations, a drop of the suspension in isopropyl alcohol was transferred onto holey carbon foils supported on conventional copper micro-grids. The ImageJ® picture analyzer software was used to estimate the mean AuNP dimensions, averaging the measurements over at least 100 data points per sample. XRD patterns were collected in the 10° - 80° angular range (step size = 0.1°; time/step = 100 s) was performed by a Philips X'Pert Pro instrument equipped with a fast X'Celerator detector, using a Cu Kα radiation-ray excitation source (40 kV, 40 mA). X-ray photoelectron spectroscopy (XPS) analyses were carried out on a Perkin Elmer Φ5600ci spectrometer using a non-monochromatized Al Kα X-ray source (1486.6 eV). Samples were mounted on stainless steel holders and introduced directly in the fast-entry lock system of the XPS analytical chamber. No sign of sample degradation due to X-ray irradiation was observed. Beside survey scans, detailed C1s, O1s, N1s, Si2p and Au4f signals were collected. The Binding Energy (BE) shifts were corrected for charging phenomena by assigning to the C1s signal of adventitious carbon a value of 284.8 eV [40]. The estimated uncertainty on for BE values was ±0.1 eV. After a Shirley-type background subtraction [54], raw spectra were fitted by adopting Gaussian–Lorentzian peak shapes, using the XPS Peak program (version 4.1, http://xpspeak.software.informer.com/4.1/, accessed February, 2019). The atomic percentages (at. %) values were evaluated using sensitivity factors provided by Φ V5.4A software.

Catalytic tests. In a typical procedure, a double neck flask was charged with a 1.0 M solution of alkyne and amine in the appropriate solvent medium and 1 % molar equivalents of Au catalyst

under nitrogen atmosphere. Tests were performed on two different volume scales (1 mL or 10 mL volume) and the amount of catalyst employed was respectively *ca*. 30 and 300 mg (the precise weight depends on the exact Au wt% content). The reaction mixture was stirred under reflux at 110 °C for the set time, then the GC-MS standard 1,3,5-TMB was added. The solid catalyst was subsequently separated from the supernatant by centrifugation (5600 rpm, 15 min) and washed three times with toluene (3 x 10 mL). Unless otherwise stated, the conversion and selectivity were determined by GC-MS analysis of an aliquot of the reaction mixture diluted in $CHCl_3$. For recycling tests, the used catalyst amount and solution volume were ≈ 300 mg and 10 mL, respectively. After the toluene washings, the exhausted catalyst was further sonicated with acetone (3 x 10 mL) for 30 min and dried in oven at 60 °C for 24 h, before being reused.

Appendix A. Supplementary Material

Additional spectroscopic and analytical data for the materials characterization and catalysis (SSNMR ^{13}CP NMR, TGA, AAS, GC-MS, XPS, TEM, GPC and ESI-MS) can be found online at https://doi.org/10.1016/j.apsusc.XXXX.XX.XXX.

Acknowlegments

The authors C.P., B.B., M.C.C., I.R., D.N., E.B. wish to thank the University of Bologna for financial support. Dr. Alberto Mucchi and Dr. Katia Rubini are gratefully acknowledged or AAS measurements, and TGA analyses, respectively.

References and Notes

[1] J. Zhao, Z. Zheng, S. Bottle, A. Chou, S. Sarina, H. Zhu, Highly efficient and selective photocatalytic hydroamination of alkynes by supported gold nanoparticles using visible light at ambient temperature, Chem. Commun. (Camb). 49 (2013) 2676–2678. doi:10.1039/c3cc38985e.

[2] T.E. Müller, K.C. Hultzsch, M. Yus, F. Foubelo, M. Tada, Hydroamination: direct addition of amines to alkenes and alkynes, Chem. Rev. 108 (2008) 3795–3892. doi:10.1021/cr0306788.

[3] S. Liang, L. Hammond, B. Xu, G.B. Hammond, Commercial supported gold nanoparticles catalyzed alkyne hydroamination and indole synthesis, Adv. Synth. Catal. 358 (2016) 3313–3318. doi:10.1002/adsc.201600804.

[4] G. Guillena, D.J. Ramón, M. Yus, Hydrogen autotransfer in the N-alkylation of amines and related compounds using alcohols and amines as electrophiles, Chem. Rev. 110 (2010) 1611–1641. doi:10.1021/cr9002159.

[5] J. J. Brunet; D. Neibecker, Catalytic Heterofunctionalization, Wiley-VCH, Weinheim, 2001.

[6] R. Severin, S. Doye, The catalytic hydroamination of alkynes., Chem. Soc. Rev. 36 (2007) 1407–20. doi:10.1039/b600981f.

[7] W. Tang, X. Zhang, New chiral phosphorus ligands for enantioselective hydrogenation, Chem. Rev. 103 (2003) 3029–3070. doi:10.1021/cr020049i.

[8] G. Desimoni, G. Tacconi, Heterodiene syntheses with α,β-unsaturated carbonyl compounds, Chem. Rev. 75 (1975) 651–692. doi:10.1021/cr60298a001.

[9] A.C. Silvanus, A. Bayle, J.R. Giguere, C. Alayrac, K. Jouvin, C. Theunissen, I.E. Wrona, O. Delacroix, G. Evano, J. Gatignol, A.-C. Gaumont, Metal-catalyzed synthesis of hetero-substituted alkenes and alkynes, Tetrahedron. 70 (2013) 1529–1616. doi:10.1016/j.tet.2013.11.073.

[10] L.J. Goossen, L. Huang, M. Arndt, K. Goossen, H. Heydt, Late transition metal-catalyzed hydroamination and hydroamidation, Chem. Rev. 115 (2015) 2596–2697. doi:10.1021/cr300389u.

[11] B. Schlummer, J.F. Hartwig, Brønsted acid-catalyzed intramolecular hydroamination of protected alkenylamines. Synthesis of pyrrolidines and piperidines, Org. Lett. 4 (2002) 1471–1474. doi:10.1021/ol025659j.

[12] I. Dion, A.M. Beauchemin, Asymmetric Brønsted acid catalysis enabling hydroaminations of dienes and allenes, Angew. Chemie - Int. Ed. 50 (2011) 8233–8235. doi:10.1002/anie.201102408.

[13] X. Cheng, Y. Xia, H. Wei, B. Xu, C. Zhang, Y. Li, G. Qian, X. Zhang, K. Li, W. Li, Lewis acid catalyzed intermolecular olefin hydroamination: scope, limitation, and mechanism, European J. Org. Chem. (2008) 1929–1936. doi:10.1002/ejoc.200701080.

[14] P.W. Roesky, T.E. Müller, Enantioselective catalytic hydroamination of alkenes, Angew. Chemie - Int. Ed. 42 (2003) 2708–2710. doi:10.1002/anie.200301637.

[15] M.T. Herrero, J.D. De Sarralde, R. Sanmartin, L. Bravo, E. Domínguez, Cesium carbonate-promoted hydroamidation of alkynes: Enamides, indoles and the effect of iron(III) chloride, Adv. Synth. Catal. 354 (2012) 3054–3064. doi:10.1002/adsc.201200430.

[16] M. Joshi, R. Tiwari, A.K. Verma, Regioselective preferential nucleophilic addition of N-heterocycles onto haloarylalkynes over N-arylation of aryl halides, Org. Lett. 14 (2012) 1106–1109. doi:10.1021/ol203491p.

[17] K.C. Hultzsch, Transition metal-catalyzed asymmetric hydroamination of alkenes (AHA), Adv. Synth. Catal. 347 (2005) 367–391. doi:10.1002/adsc.200404261.

[18] K.C. Hultzsch, Catalytic asymmetric hydroamination of non-activated olefins, Org. Biomol. Chem. 3 (2005) 1819–1824. doi:10.1039/b418521h.

[19] I. Aillaud, J. Collin, J. Hannedouche, E. Schulz, Asymmetric hydroamination of non-activated carbon-carbon multiple bonds, Dalton Trans. 33 (2007) 5105–5118. doi:10.1039/b711126f.

[20] A. Grirrane, H. Garcia, A. Corma, E. Álvarez, Air-stable, dinuclear and tetranuclear σ,π-acetylide gold(I) complexes and their catalytic implications, Chem. - A Eur. J. 19 (2013) 12239–12244. doi:10.1002/chem.201301623.

[21] A. A. Corma, A. Leyva-Pérez, M.J. Sabater, Gold-catalyzed carbon−heteroatom bond-forming reactions, Chem. Rev. 111 (2011) 1657–1712. doi:10.1021/cr100414u.

[22] A.S.K. Hashmi, G.J. Hutchings, Gold catalysis, Angew. Chemie - Int. Ed. 45 (2006) 7896–7936. doi:10.1002/anie.200602454.

[23] A.S.K. Hashmi, Gold-catalyzed organic reactions, Chem. Rev. 107 (2007) 3180–3211. doi:10.1007/3418-2012-45.

[24] A. Corma, P. Concepción, I. Domínguez, V. Forné, M.J. Sabater, Gold supported on a biopolymer (chitosan) catalyzes the regioselective hydroamination of alkynes, J. Catal. 251 (2007) 39–47. doi:10.1016/j.jcat.2007.07.021.

[25] L.C. Lee, Y. Zhao, Room temperature hydroamination of alkynes catalyzed by gold clusters in interfacially cross-linked reverse micelles, ACS Catal. 4 (2014) 688–691. doi:10.1021/cs401213c.

[26] V.A. Solovyeva, K.B. Vu, R. Sougrat, V.O. Rodionov, One-pot synthesis of Au@SiO_2 catalysts: a click chemistry approach, ACS Comb. Sci. 16 (2014) 513−517. doi: 10.1021/co5000932.

[27] A. Seral-Ascaso, A. Luquin, M.J. Lázaro, G.F. De La Fuente, M. Laguna, E. Muñoz, Synthesis and application of gold-carbon hybrids as catalysts for the hydroamination of alkynes, Appl. Catal. A Gen. 456 (2013) 88–95. doi:10.1016/j.apcata.2013.02.008.

[28] B. Ballarin, D. Barreca, E. Boanini, M.C. Cassani, P. Dambruoso, A. Massi, A. Mignani, D. Nanni, C. Parise, A. Zaghi, Supported gold nanoparticles for alcohols oxidation in continuous-flow heterogeneous systems, ACS Sustain. Chem. Eng. 5 (2017) 4746–4756. doi:10.1021/acssuschemeng.7b00133.

[29] M.C. Cassani, A. Migliori, B. Ballarin, D. Nanni, D. Barreca, A. Riminucci, I. Bergenti, V. Morandi, E. Boanini, G. Carraro, C. Parise, Structure, morphology and magnetic properties of Au/Fe_3O_4 nanocomposites fabricated by a soft aqueous route, Ceram. Int. 45 (2019) 449–456. doi:10.1016/j.ceramint.2018.09.188.

[30] A.P. Legrand, ed., The Surface Properties of Silica, Wiley-VCH, Weinheim, Germany, 1998.

[31] M. C. Pirrung, The Synthetic Organic Chemist’s Companion, Wiley, 2007.

[32] K. Hara, S. Akahane, J.W. Wiench, B.R. Burgin, N. Ishito, V.S.Y. Lin, A. Fukuoka, M. Pruski, Selective and efficient silylation of mesoporous silica: A quantitative assessment of synthetic strategies by solid-state NMR, J. Phys. Chem. C. 116 (2012) 7083–7090. doi:10.1021/jp300580f.

[33] M. V. Zakharova, N. Masoumifard, Y. Hu, J. Han, F. Kleitz, F.G. Fontaine, Designed synthesis of mesoporous solid-supported Lewis acid-base pairs and their CO_2 adsorption behaviors, ACS Appl. Mater. Interfaces. 10 (2018) 13199–13210. doi:10.1021/acsami.8b00640.

[34] S. Fazzini, M.C. Cassani, B. Ballarin, E. Boanini, J.S. Girardon, A.-S. Mamede, A. Mignani, D. Nanni, Novel synthesis of gold nanoparticles supported on alkyne-functionalized nanosilica, J. Phys. Chem. C. 118 (2014) 24538–24547. doi:10.1021/jp507637m.

[35] B. Ballarin, D. Barreca, E. Boanini, E. Bonansegna, M.C. Cassani, G. Carraro, S. Fazzini, A. Mignani, D. Nanni, D. Pinelli, Functionalization of silica through thiol-yne radical chemistry: a catalytic system based on gold nanoparticles supported on amino-sulfide-branched silica, RSC Adv. 6 (2016) 25780–25788. doi:10.1039/C6RA02479C.

[36] J.F. Moulder, W.F. Stickle, P.E. Sobol, K.D. Bomben, Handbook of X-ray photoelectron spectroscopy, (1992) 261. doi:10.1002/sia.740030412.

[37] http://srdata.nist.gov/xps/.

[38] M. Sengupta, A. Bag, S. Das, A. Shukla, L.N.S. Konathala, C.A. Naidu, A. Bordoloi, Reaction and mechanistic studies of heterogeneous hydroamination over support-stabilized gold nanoparticles, ChemCatChem. 8 (2016) 3121–3130. doi:10.1002/cctc.201600762.

[39] A. Gasparotto, S. Polizzi, E. Tondello, L. Armelao, D. Barreca, E. Pierangelo, Preparation of gold nanoparticles on silica substrate by radio frequency sputtering, J. Nanosci. Nanotechnol. 5 (2005) 259–265. doi:10.1166/jnn.2005.027.

[40] D. Briggs, M.P. Seah, Practical surface analysis: Vol. 1, Auger and X-ray photoelectron spectroscopy, Wiley, New York, 1990.

[41] K.I. Fujita, A. Fujii, J. Sato, H. Yasuda, Magnetically recoverable N-heterocyclic carbene-gold(I) catalyst for hydroamination of terminal alkynes, Synlett. 27 (2016) 1941–1944. doi:10.1055/s-0035-1562134.

[42] J.E. Perea-Buceta, T. Wirtanen, O.V. Laukkanen, M.K. Mäkelä, M. Nieger, M. Melchionna, N. Huittinen, J.A. Lopez-Sanchez, J. Helaja, Cycloisomerization of 2-alkynylanilines to indoles catalyzed by carbon-supported gold nanoparticles and subsequent homocoupling to 3,3'-biindoles, Angew. Chemie - Int. Ed. 52 (2013) 11835–11839. doi:10.1002/anie.201305579.

[43] Y.P. He, H. Wu, D.F. Chen, J. Yu, L.Z. Gong, Cascade hydroamination/redox reaction for the synthesis of cyclic aminals catalyzed by a combined gold complex and Brönsted acid, Chem. - A Eur. J. 19 (2013) 5232–5237. doi:10.1002/chem.201300052.

[44] E. Mizushima, T. Hayashi, M. Tanaka, Au(I)-catalyzed highly efficient intermolecular hydroamination of alkynes, Synthesis (Stuttg). 5 (2003) 3349–3352. doi:10.1021/ol0353159.

[45] Variable amounts of acetophenone were usually observed, by all authors, in hydroaminations of phenylaceteylene with aniline. When selectivities are low it normally means that acetophenone is formed. This side-product could in principle arise both/either from hydrolysis of the resulting imine and/or hydration of the alkyne. Control experiments confirmed that the latter reaction actually occurs, but it is very slow. Hence, the small amounts of acetophenone observed in our reactions result from hydrolysis of the imine. No significant amounts of other by-products were obtained.

[46] J. Vohlídal, J. Sedláček, J. Rathouský, J. Svoboda, N. Žilková, H. Balcar, Hybrid Catalysts for acetylenes polymerization prepared by anchoring $[Rh(cod)Cl]_2$ on MCM-41, MCM-48 and SBA-15 mesoporous molecular sieves - The Effect of support structure on catalytic activity in polymerization of phenylacetylene and 4-ethynyl-N-{4-[(trimethylsilyl)-ethynyl]benzylidene}aniline, Collect. Czechoslov. Chem. Commun. 68 (2003) 1861–1876. doi:10.1135/cccc20031861.

[47] K. Freitag, J. Gracia, A. Martín, M. Mena, J.-M. Poblet, J.P. Sarasa, C. Yelamos, Rhodium/ Iridium-Titanium Azaheterometallocubanes, Chem. Eur. J. (2001) 3644–3651. doi: 10.1002/1521-3765(20010903)7

[48] H. Katayama, K. Yamamura, Y. Miyaki, F. Ozawa, Stereoregular polymerization of phenylacetylenes catalyzed by [hydridotris(pyrazolyl)borato]rhodium(I) complexes, Organometallics. 16 (1997) 4497–4500. doi:10.1021/om9703090.

[49] J. Sedláček, M. Pacovská, D. Rédrová, H. Balcar, A. Biffis, B. Corain, J. Vohlídal, Polybenzimidazole-supported $[Rh(cod)Cl]_2$ complex: Effective catalyst for the polymerization of substituted acetylenes, Chem. - A Eur. J. 8 (2002) 366–371. doi:10.1002/1521-3765(20020118)8.

[50] V. Durà-Vilà, D.M.P. Mingos, R. Vilar, A.J.P. White, D.J. Williams, Reactivity studies of $[Pd,(\mu\text{-}X)_2(PBu_3^t)_2]$ (X = Br, I) with CNR (R = 2,6-dimethylphenyl), H_2 and alkynes, J. Organomet. Chem. (2000) 198–205.

[51] G. Braurer, Handbook of Preparative Inorganic Chemistry, Academic Press: New York, 1963.

[52] W.L.F. Armarego, Purification of Laboratory Chemicals, 8th ed., Elsevier Inc., Oxford, 2017.

[53] J. Manna, B. Roy, P. Sharma, Efficient hydrogen generation from sodium borohydride hydrolysis using silica sulfuric acid catalyst, J. Power Sources. 275 (2015) 727–733. doi:10.1016/j.jpowsour.2014.11.040.

[54] D.A. Shirley, High-resolution X-Ray photoemission spectrum of the valence bands of Gold, Phys. Rev. B. 5 (1972) 4709.